

Article

Quantitative Evaluation of Complex Degree of Geological Structure in Yangquan Mining Area

Yang Pu ^{1,2,*} and Zhihua Yang ³

¹ State Key Laboratory of the Gas Disaster Detecting, Preventing and Emergency Controlling, Chongqing 400037, China

² China Coal Technology Engineering Group Chongqing Research Institute, Chongqing 400039, China

³ Huayang New Material Technology Group Co., Ltd., Yangquan 045000, China

* Correspondence: puyang_0429@126.com

Abstract: The study and analysis of tectonic activities on regional structures is of great significance to mine prospecting and production safety in mine work. We take the No. 3 coal seam in the Yangquan mining area as the object of study. The methods of fractal dimension, structural curvature and trend surface analysis are applied to quantitatively evaluate and predict the mine structure. The folded meso-plane analysis is also carried out. The results show that the trend surface reflects that the monoclinic structure is high in the NE direction and low in the SW direction. The dip angle is small, and the overall structure is characterized by an NNE–NE trend. The curvature value of the coal seam in the mining area is generally small. The northwest structure is relatively simple. The eastern fracture is more developed. The southern structure is relatively simple. A large nearly EW direction Taohe syncline is developed in the middle and south. Several large fractures in the NE direction are developed in the southwest. The capacity dimension of fractures in the mine field is mostly between 0.6 and 1.6. It indicates that the complexity of the fracture structure in the mine field has obvious heterogeneity. The neutral surface of the mine is in the third section of Taiyuan formation, and the No. 3 coal seam is above it. The research results have reference significance for the evaluation and prediction of safe mining and gas outburst danger zones in mining areas.

Keywords: geological structure; trend surface; curvature; constructing fractal; neutral plane



Citation: Pu, Y.; Yang, Z.

Quantitative Evaluation of Complex Degree of Geological Structure in Yangquan Mining Area. *Sustainability* **2022**, *14*, 12028. <https://doi.org/10.3390/su141912028>

Academic Editors: Haiyan Wang, Jia Lin and Guojun Zhang

Received: 15 August 2022

Accepted: 19 September 2022

Published: 23 September 2022

Publisher's Note: MDPI stays neutral with regard to jurisdictional claims in published maps and institutional affiliations.



Copyright: © 2022 by the authors. Licensee MDPI, Basel, Switzerland. This article is an open access article distributed under the terms and conditions of the Creative Commons Attribution (CC BY) license (<https://creativecommons.org/licenses/by/4.0/>).

1. Introduction

Fracture and fold are the main geological structures that affect the safety of mine production. The comprehensive evaluation of the structural complexity of the mining area is of great significance for safe mining, high yield and efficiency and optimization of production deployment [1–3]. In the present circumstances, the comprehensive evaluation of the complexity of structural development can only achieve the quantitative description of a single factor. It cannot reflect the complexity and the variation trend of the structure in general [4–7]. In particular, the complexity of the structure can only be qualitatively described in areas where multiple structural forms coexist.

For the study of the evaluation and prediction of mine structures, the structural index method was proposed by former West German mining and geological workers in the early 1980s as a representative [8]. In China, Zhan et al. [9] put forward the qualitative or semi-quantitative method called “equal block method” with limited evaluation accuracy. Xu et al. [10] first applied the fuzzy comprehensive evaluation method to study the relative complexity of mine structures. Xia et al. [11] introduced the gray correlation analysis method into fuzzy comprehensive evaluation. They used the normalized correlation degree to replace the factor weight in the fuzzy comprehensive evaluation, so as to realize the automatic assignment of the weight set and computerization of the fuzzy comprehensive evaluation process. In the quantitative prediction of the complexity of mine structures, Xia et al. [12,13] combined self-organizing modeling technology with the

artificial neural network method to carry out index prediction and quantitative prediction of mine structures.

In terms of the application of geological structures in mines, Zhu et al. [14,15] took the Nantong mining area as an example to analyze the distribution characteristics of coal metamorphism and coal failure degree from the perspective of tectonic and tectonic stress field evolution. Zhang et al. [16–18] studied the tectonic evolution characteristics of the Pingdingshan, Suxian and Xinmi mining areas from the perspective of regional tectonic evolution. Song et al. [19] pointed out that coalbed methane enrichment was controlled by tectonic evolution. Taking the Fuxin mining area as an example, Han et al. [20] pointed out the regional distribution of local tectonic stress, tectonic coal and gas in a multi-stage evolution of the tectonic stress field, so as to control the zoning of mine dynamic disasters. Zhang et al. [21,22] put forward the theory of gradual control of gas occurrence structure, which laid the foundation for revealing the mechanism of gas occurrence distribution and gas outburst in coal mines in China. In addition, some scholars related to geological structure and evolution, formation and distribution of tectonic coal, coal petrological characteristics and structure of tectonic coal and its influence on gas occurrence and gas outburst carried out more in-depth analyses and discussions [23–29].

Tectonic activities provide energy for mineralization and control the mineralization zoning. Over the years, the qualitative research on the control effect of geological structures on the occurrence conditions of coal seam has been deeply understood [30–36], but the quantitative relationship between them is still under exploration. Some scholars have carried this out such as the use of regression analysis, gray correlation [37,38], the artificial neural network based on fault fractal information dimension of evaluation of mine geological structure, which is relatively complex [39], the degree of coal floor contour structure curvature [40] and other research, trying to use the method of quantitative evaluation, the study of geological structures of coal seam occurrence condition control. However, in the quantitative evaluation index of geological structures, there are still some problems such as not accurate assignments or not comprehensive considerations.

The research and analysis of regional structures are of great significance to mine prospecting and production safety in mine work. Yangquan mining area is a high-gas mining area, and gas geological disasters are the main factors threatening the safe and efficient production of the mining area. Based on that, this paper takes the No. 3 coal seam in the Yangquan mining area as the research object, quantitatively analyzes and evaluates the structural complexity of the Yangquan mining area by using mathematical analysis methods. The research results not only have a more in-depth understanding of the folds, fractures, collapse columns and distribution of groundwater in the Yangquan mining area, but also provide strong data support for the next mining activities in the Yangquan mining area. It also has reference significance to guide the optimization of mining deployment in the later stage of the mine and the auxiliary coal and gas outburst dangerous area division. In addition, the research method can also be used for reference to other mining areas.

2. Mine Structural Characteristics

The mining area is located in the Zhanshang-Wuxiang-Yangcheng NNE direction fold belt on the northeast edge of Qinshui Basin. The eastern part is the Taihang Mountain uplift belt. The western and northwestern parts are the Taiyuan Basin. The northern part is the 38° EW direction tectonic subzone. This area is controlled by the uplift of Taihang Mountain in the east and Wutai Mountain in the north. The structural morphology is generally characterized by large irregular monoclinic structure with NW direction and SW direction. The dip angle of strata is relatively slow, generally about 10°. The secondary wide and slow multi-stage superimposed folds constitute the main structural morphology of the Yangquan mining area. There are only large fractures sparsely developed in the south of the mining area, which are generally dominated by small normal fractures. The development of collapse columns is relatively dense. The main coal seam is the No. 3 coal seam. The contour and structure of the bottom plate are shown in Figure 1.

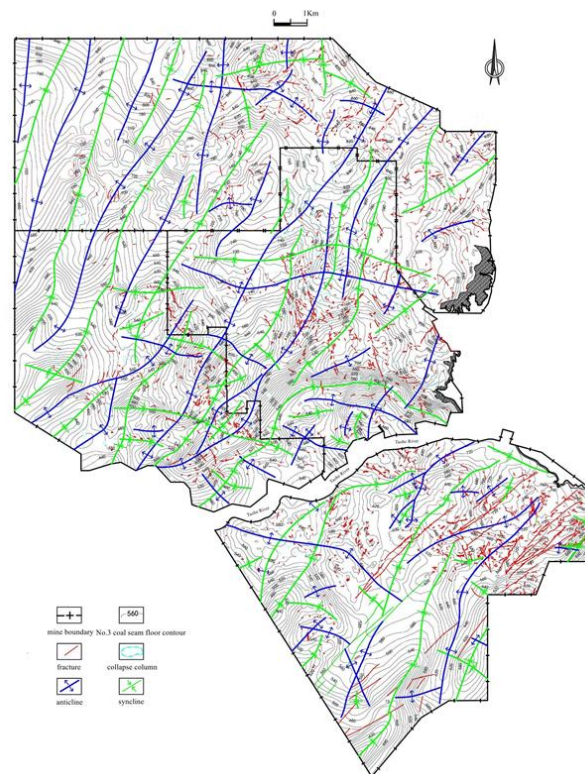


Figure 1. Contour and structure outline map of No. 3 coal seam floor.

3. Structural Trend Surface Analysis

Trend surface analysis is a method to study and analyze the spatial analysis of geological features. It approximates the spatial distribution of geological features by the surface represented by some form of function. The mining area is dominated by gentle multi-directional and multi-period fold structures, lacking large fractures. It is near continuous surface in space and has good stratigraphic continuity. So, it is suitable to analyze its characteristics by using trend surface.

3.1. Trend Surface Analysis

3.1.1. Trend Surface and Its Analysis

The observed values of geological variables (X_{ground}) can be divided into trend part (X_{area}) and residual part (X_{residual}) by mathematical methods. The latter can be divided into local residual (X_{local}) and random residual (X_{random}). The following expression is as follows:

$$X_{\text{ground}} = X_{\text{area}} + X_{\text{local}} + X_{\text{random}} \quad (1)$$

In the formula, X_{ground} is observation values of geological variable, X_{area} is regional component and is also called trend value, X_{local} is local variation component and X_{random} is component of random variation.

3.1.2. Types of Trend Surface Analysis

Polynomial trend surface analysis is widely used in coalfield geological work. When the degree of polynomial increases, it can approximate any continuous function. The two-dimensional trend surface analysis is commonly used in geology.

3.1.3. Theory of Calculation

For a geological variable, there are “ i ” observation points on the plane and “ n ” corresponding observation values “ z_i ”. With the different position of observation points, the

observation values also change accordingly. It indicates that there is a correlation between the two, and the expression is:

$$z = f(x, y) \quad (2)$$

The three data z_i, x_i, y_i of each observation point constitute the basic data of trend surface analysis. For a trend surface, the equation is:

$$z_i = b_0 + b_1x_i + b_2y_i \quad (3)$$

For the P-th trend surface analysis, the trend surface equation is:

$$z_i = b_0 + b_1x_i + b_2y_i + b_3x_i^2 + b_4x_iy_i + b_5y_i^2 + \dots + b_ky_i^P \quad (4)$$

$K = P(P + 3)/2$, $k + 1$ is the number of coefficients to be determined.

3.2. Trend Surface Analysis Results

Based on the floor contour line of No. 3 coal seam in the mining area, the floor elevation of coal seam is selected as the geological variable. The trend surface and residual analysis of coal seam are carried out one to four times. Through the analysis of the trend and residual variation in the coal seam, we discussed the development law of geological structures after coal formation. In the regional scope, 971 boreholes in No. 3 coal seam were collected. In order to improve the accuracy of trend surface analysis, 7003 points were evenly taken along the contour of the coal seam floor and 7974 data points were collected for trend surface and residual analysis.

3.2.1. Explicitness Test and Results

In trend surface analysis, "F" distribution test and fitting "N_c" are generally used to test the significance of the analysis results.

1. Total coefficient test

The whole coefficient test of the trend surface equation is to test whether the linear correlation between geological variables (z) and independent variables as well as their higher power and cross product power is obvious.

$$F = (S_{\text{regression}}/k)/[S_{\text{random}}/(n - 1 - k)] \quad (5)$$

In the formula, $S_{\text{regression}}$ is the sum of squares of regression deviation which represents the systematic error caused by independent variables. S_{residue} is the residual deviation sum which represents the error caused by local and uncontrolled factors.

Given the explicitness level F_a , if $F < F_a$, the trend surface is not explicit. On the contrary, the linear correlation between dependent variables and independent variables is considered, and the trend surface equation is obvious.

2. Trend surface fitting

The trend face of the approximation of the original data can be expressed by the change in the sum of squares of deviations in mathematics. The higher the fitting degree, the better the fitting degree of the trend surface.

$$N_c = S_{\text{regression}}/S_{\text{total}} \times 100\% \quad (6)$$

In the formula, S_{total} is total variance sum of trend surfaces.

The test results are as follows: the number of samples of No. 3 coal seam is $n = 7974$, and the F critical value of each trend surface of each coal seam is obtained by looking up the F distribution table: first $F_{0.05}(2, 7971) < F_{0.05}(2, 1000) = 3$; second $F_{0.05}(5, 7968) < F_{0.05}(5, 1000) = 2.22$; third $F_{0.05}(9, 7964) < F_{0.05}(9, 1000) = 1.89$; fourth $F_{0.05}(14, 7959) < F_{0.05}(14, 1000) = 1.7$.

The statistical results show that $F_1 = 1953.9825 > 3$, $F_2 = 1119.7502 > 2.22$, $F_3 = 791.4655 > 1.89$ and $F_4 = 772.2111 > 1.7$. Under the given significant level $\alpha = 0.05$, the one–four trend surface equations of No. 3 coal seam are very significant.

3.2.2. Trend Surface and Residual Analysis of Mine Structure

1. Trend surface analysis

Through trend surface analysis and calculation, the fitting degrees are 88.80%, 90.12%, 91.53% and 91.90%, which are better fitted with the actual situation. Drawing the data with Surfer10 software, the one to four trend surface analysis maps of No. 3 coal seam are obtained as shown in Figure 2.

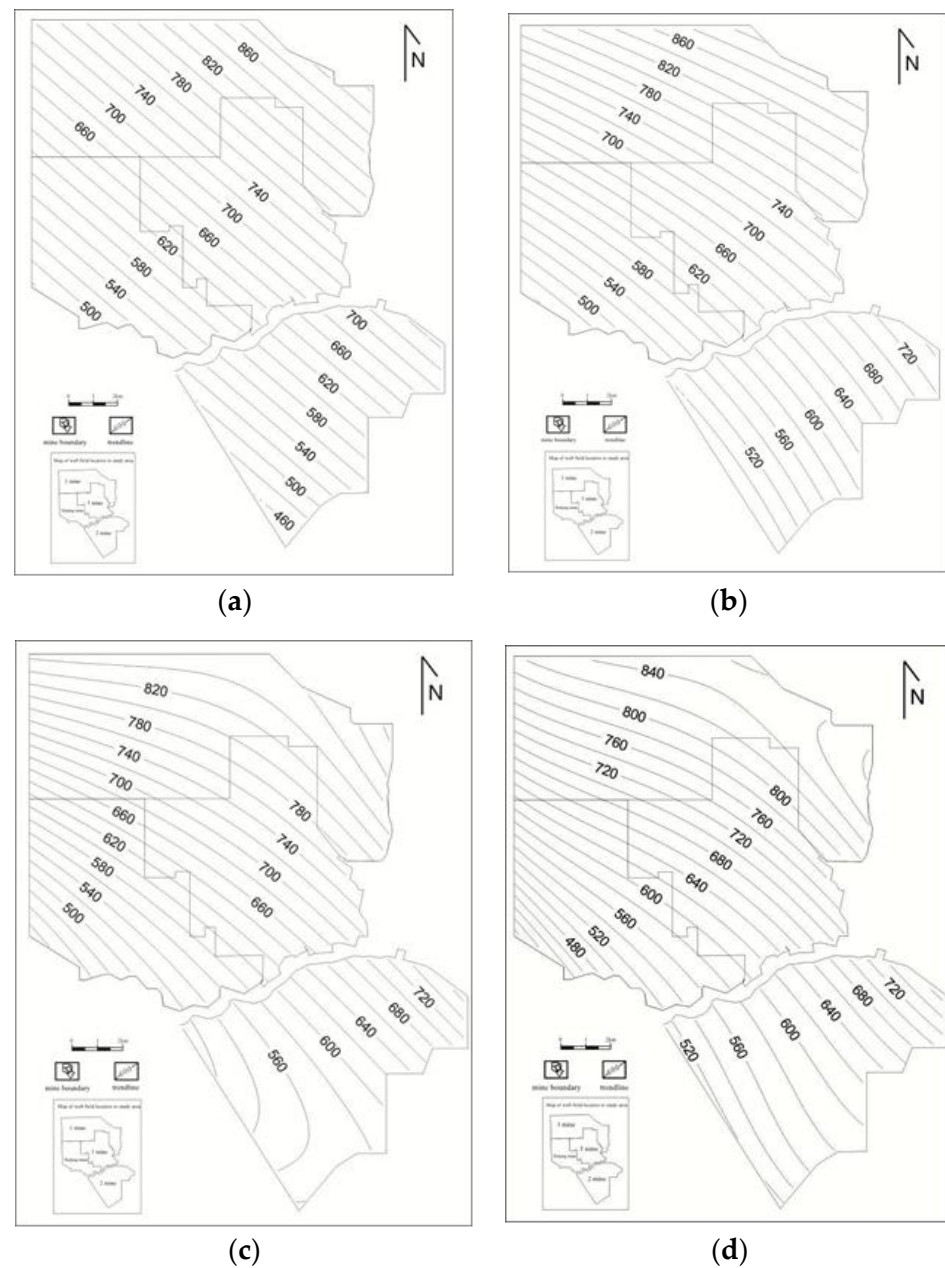


Figure 2. The 1st–4th trend surface analysis results of No. 3 coal seam. (a) Results of the 1st trend surface analysis of No. 3 coal seam. (b) Results of the 2nd trend surface analysis of No. 3 coal seam. (c) Results of the 3rd trend surface analysis of No. 3 coal seam. (d) Results of the 4th trend surface analysis of No. 3 coal seam.

The first trend surface map shows that the coal seam is a monoclinic structure high in the NE direction and low in the SW direction. The strata are generally in NW–SE trend, inclined to the SW direction. The dip angle is small. This trend is consistent with the regional tectonic background of the large monoclinic structure in the Yangquan mining area on the NE edge of Qinshui Basin, which better reflects the overall trend of the strata in the mining area. It can be seen from the comparison between the second trend surface map and the first trend surface that the overall trend of the coal seam inclined to the SW direction is unchanged. The overall trend shows a wide and gentle oblique trend protruding to the NE direction, which reflects the overall shape of the target coal seam located in the NE edge of the Qinshui Basin, and the overall structural direction is NE.

It can be seen from the third and fourth trend surface maps that the coal seam contour is generally characterized by gentle undulation. The strata generally tend toward the SW direction. The overall structural direction is still the NE direction. At the same time, the fourth trend surface map with the highest fitting degree shows that the NE edge of the study area has the characteristics of a sub-level NW-trending wide and gentle anticline. It indicates that the overall mining area is dominated by NE direction folds, followed by NW direction folds.

It can be seen that the residual values are in good agreement with the folds in the mining area after analyzing the first–fourth residual maps. The syncline is negative, and the anticline is positive. The residual change caused by structural superposition is very obvious. With the increase in fitting (N_c), the high-order residual map shows the structural morphology of the study area more clearly and in detail. The fourth order residual map is more obvious than the first order residual map, which is mainly manifested in the western part of the study area. For example, the Lujiashuang anticline and the Huyuxi syncline in Shiziping show a negative and positive trend in the fourth order residual map, while the first order residual map is all above the line zero. Other places, such as Fowa anticline, northeast edge area and S_{15} syncline of No. 2 Coal Mine, also have similar situations.

It is considered that the fourth residual map can more accurately reflect the overall shape of the mining area and show the development scale of folds through the comparison of first–fourth trend faces. It shows that the strata in the mining area have developed more folds on the monoclinic structure tilted toward the SW direction as a whole. The folds are mainly distributed in the NNE–NE trend and large-scale in the axial direction, which controls the basic morphology of the mining area. On this basis, the secondary, small EW direction and NW direction folds are developed. The dome and tectonic basin are formed by the superposition and transformation of folds in different periods. The residual value of the superposition part of the structure has a certain mutation, which reflects the structural morphology of the mining area under the action of multiple tectonic movements. At the same time, the residual analysis shows the fold morphology in different structural zones more clearly. The western part of the mining area is dominated by large-scale folds, the development scale of syncline is larger than that of syncline and the morphology of the central superimposed fold area is also obvious.

2. Residual analysis

Figure 3 shows the residual analysis of mining areas first–fourth. In the residual plot, red lines are used to mark the isoline with a residual value of zero. By comparison, it is consistent with the contour of the coal seam floor. The residual map shows the overall structural characteristics of the mining area. The secondary fold developed on the SW inclined monoclinic structure is the main structural form. However, by distinguishing the positive and negative values, the latter more clearly depicts the development of anticlines and synclines, and is more clear for analyzing the development scale and influencing range of folds.

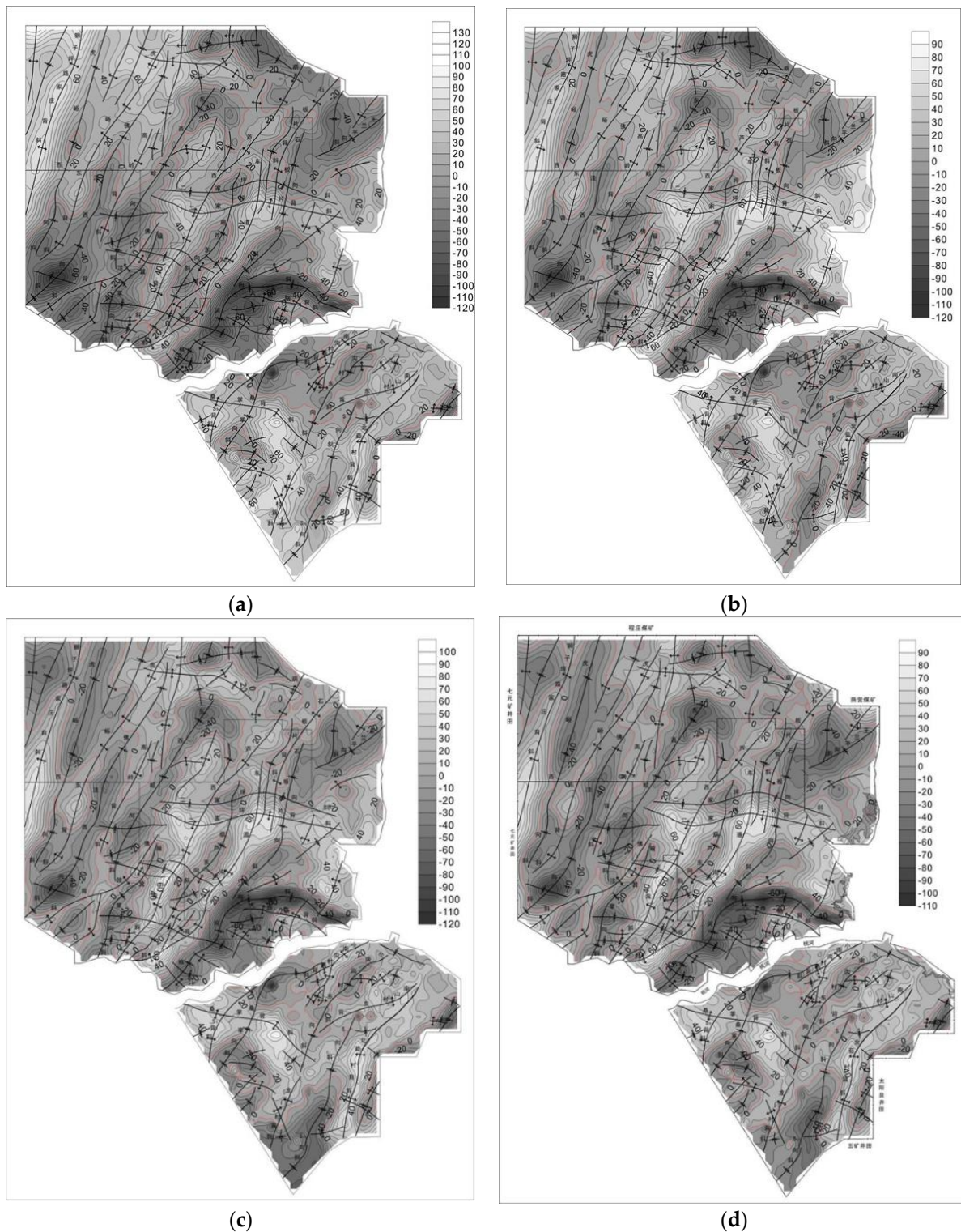


Figure 3. The 1st–4th residuals and fold distribution map of No. 3 coal seam. (a) First residual and fold distribution map of No. 3 coal seam. (b) Second residual and fold distribution map of No. 3 coal seam. (c) Third residual and fold distribution map of No. 3 coal seam. (d) Fourth residual and fold distribution map of No. 3 coal seam.

4. Curvature Analysis

The main structures in the study area are mainly folds. Its stratigraphic continuity is good. The fracture is small or not developed. The structural curvature method is an effective

method for the quantitative study of folds. According to the basic concept of curvature, it can be divided into principal curvature, mean curvature and Gaussian curvature.

4.1. Calculation Method of Curvature

There are many methods for calculating the curvature value of a complex deformation surface [40]. According to the actual situation of the mine, this paper takes the contour of the actual coal seam floor as the base map to grid the coal level and calculate the curvature.

When calculating the curvature of a certain point, the local quadratic surface is fitted by the least square method and the 3×3 mesh unit is used for approximation, as shown in Figure 4. According to the definition of the first and second derivatives in calculus mathematics, the coefficients in Equations (7)–(13) are obtained:

$$z = ax^2 + by^2 + cxy + dx + ey + f \quad (7)$$

$$a = \frac{1}{2} \times \frac{\partial^2 z}{\partial x^2} = \frac{z_1 + z_3 + z_4 + z_6 + z_7 + z_9}{12\Delta x^2} - \frac{z_2 + z_5 + z_8}{6\Delta x^2} \quad (8)$$

$$b = \frac{1}{2} \times \frac{\partial^2 z}{\partial y^2} = \frac{z_1 + z_2 + z_3 + z_7 + z_8 + z_9}{12\Delta x^2} - \frac{z_4 + z_5 + z_6}{6\Delta x^2} \quad (9)$$

$$c = \frac{\partial^2 z}{\partial x \partial y} = \frac{z_3 + z_7 - z_1 - z_9}{4\Delta x^2} \quad (10)$$

$$d = \frac{\partial z}{\partial x} = \frac{z_3 + z_6 + z_9 - z_1 - z_4 - z_7}{6\Delta x} \quad (11)$$

$$e = \frac{\partial z}{\partial y} = \frac{z_1 + z_2 + z_3 - z_7 - z_8 - z_9}{6\Delta x} \quad (12)$$

$$f = \frac{2(z_2 + z_4 + z_6 + z_8) - (z_1 + z_3 + z_7 + z_9) + 5z_5}{9} \quad (13)$$

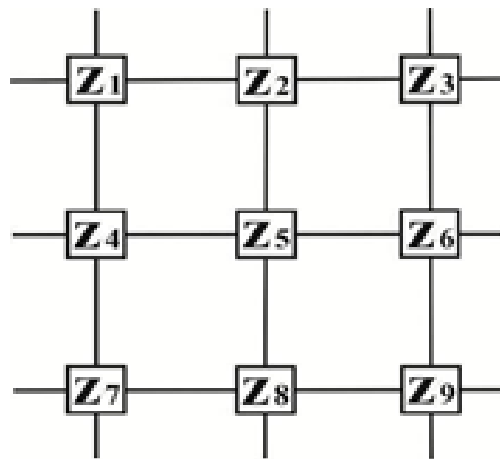


Figure 4. A 3×3 grid schematic.

In the formula: “ $Z_1 \dots Z_9$ ” is the coal seam floor elevation of the plane grid point “ Z_1 – Z_9 ” shown in the graph. “ Δx ” is the horizontal distance between grid nodes. On this basis, the average curvature “ K_m ” and Gaussian curvature “ K_g ” at the coal level can be calculated.

Average curvature:

$$K_m = - \frac{a(1 + e^2) + b(1 + d^2) - cde}{(1 + d^2 + e^2)^{3/2}} \quad (14)$$

Gaussian curvature:

$$K_g = \frac{4ab - c^2}{(1 + d^2 + e^2)^2} \quad (15)$$

4.2. Analysis of Curvature

On the contour map of No. 3 coal seam in the Yangquan mining area, a point is taken every 250 m. The geographic coordinate (X, Y) is recorded and elevation data Z of the point are plotted into tables. A total of 3822 points are taken. In addition to the boundary points and invalid points, the coordinates of the remaining effective points are used to calculate the maximum curvature value, the minimum curvature value, the Gaussian curvature value and the average curvature value. The maximum curvature map (Figure 5), the minimum curvature map (Figure 6), the average curvature map (Figure 7) and the Gaussian curvature map (Figure 8) are obtained.

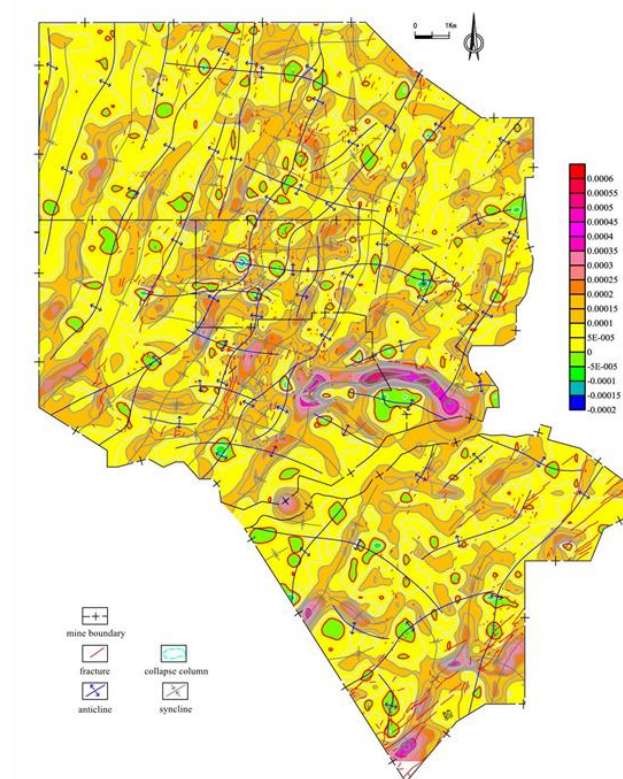


Figure 5. Maximum curvature map of No. 3 coal seam in Yangquan mining area.

4.2.1. Maximal Curvature and Minimal Curvature

The study area is located on the northeast edge of Qinshui Basin, and the deformation degree of the coal seam is small, corresponding to the maximum and minimum curvatures of the study area in the figure (−0.00048, 0.00012). The curvature values of the maximum curvature diagram and the minimum curvature diagram are relatively small. It indicates that the bending degree of the coal seam is relatively small. It is consistent with the small inclination angle of the actual coal seam. On the whole, the contour lines in the figure are mainly distributed between positive and negative phases in the NNW–SSE trend and extend along the NNE direction. It indicates that the No. 3 coal seam folds in this area are mainly arranged between anticlines and synclines in the NNE direction, and the contour lines are extremely dense near the axis trace. It indicates that the coal seam elevation changes greatly, which well reflects the fold characteristics in this area. Among them, there are some NNW direction and near EW direction extensions of the contour lines, indicating

that the area on the basis of NNE direction fold also developed some NNW direction and near EW direction secondary folds.

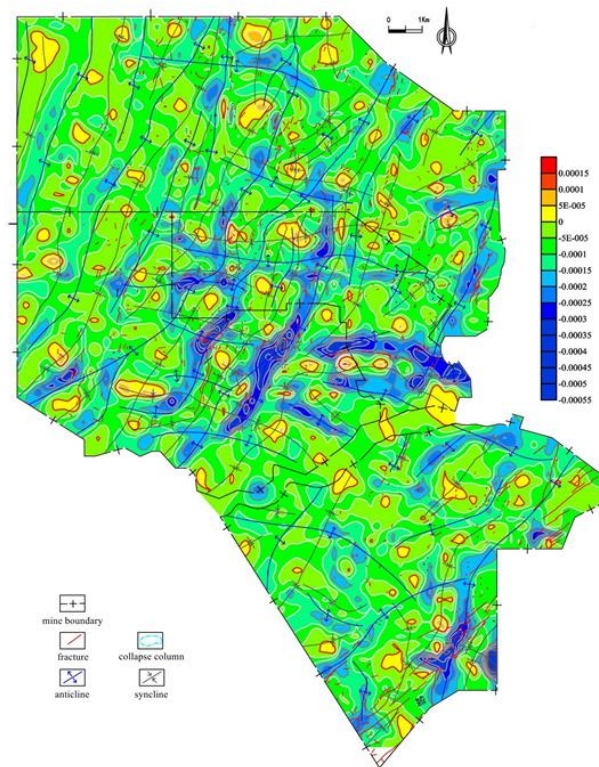


Figure 6. Minimum curvature map of No. 3 coal seam in Yangquan mining area.

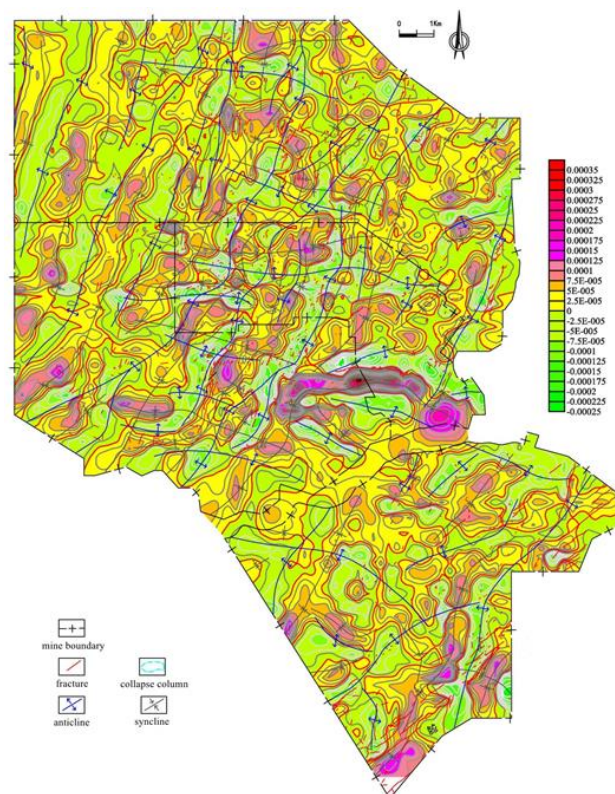


Figure 7. Average curvature diagram of No. 3 coal seam in Yangquan mining area.

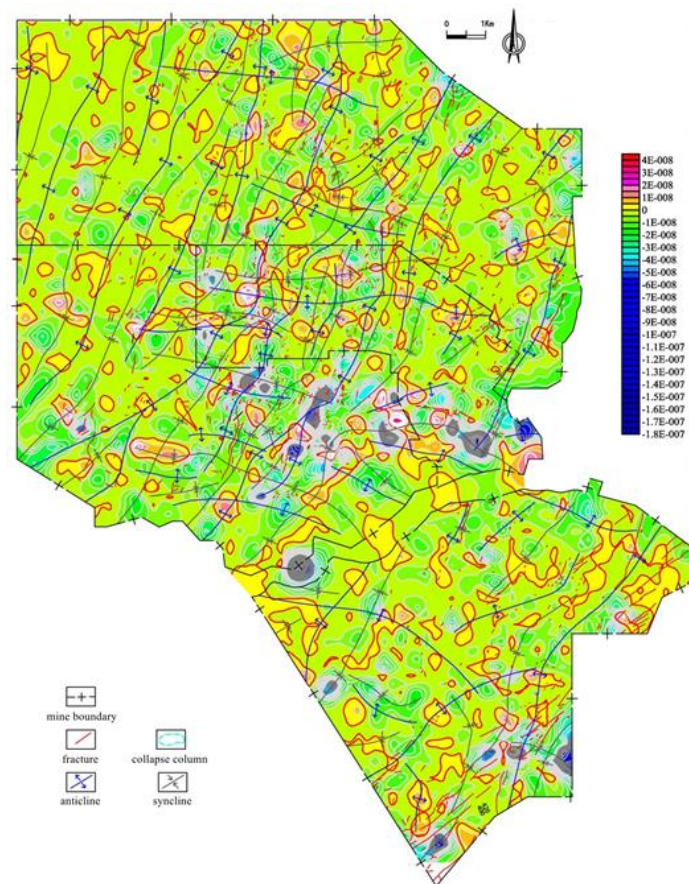


Figure 8. Gaussian curvature diagram of No. 3 coal seam in Yangquan mining area.

By comparison of two graphs, the distribution of isolines in two graphs has obvious similarity. On the whole, the curvature values in the western and northern regions are generally small, and the variation range is not large. The maximum curvature is concentrated in 0.00005, and the minimum curvature is concentrated in -0.005 . The contour lines are relatively sparse, and they are distributed in strips. The variation range of the eastern curvature value increases significantly. The maximum curvature of some regions is as high as 0.00025, and the minimum curvature is as low as -0.00025 . The overall maximum curvature and minimum curvature in the south have little change, and the curvature value is similar to that in the northwest. However, the maximum curvature and minimum curvature in the southeast region have obvious changes. The maximum curvature in the local region can reach 0.00045, and the minimum curvature can reach -0.0004 .

The structure northwest of the study area is relatively simple and the deformation is weak. The eastern fracture is relatively developed, which has great influence on the maximum and minimum curvatures. The coal seam has a certain deformation and is in the weak fold deformation area. In the south-central part, there is a large near EW direction Taohe syncline with strong superimposed deformation, which has certain influence on the surrounding area. It leads to great variation in the maximum curvature and minimum curvature and obvious deformation of the coal seam. The southern structure is relatively simple. Some large folds are developed, and the maximum and minimum curvature changes are relatively small. However, several large NE direction fractures are developed in the southwest, which have a great influence on the maximum and minimum curvatures of the surrounding areas.

4.2.2. Average Curvature

It can be seen from the figure that the directions of anticline and syncline are consistent with the extension direction of the same contour line in the curvature figure. It fully illustrates that the average curvature has a good indication effect on the anticline and syncline in the Yangquan mining area.

The value range of average curvature is between -0.00024 and 0.00032 , and the curvature value is relatively small. The average curvature of most areas is concentrated around 4×10^{-5} . It indicates that the bending degree of the coal seam is relatively small. It is consistent with the small inclination of the actual coal seam. In the average curvature map, the curvature value in the northwest is generally small and the change range is not large. The average curvature interval is between -0.000025 and 0.000025 , and the contour is striped and equidistant. The variation range of the eastern curvature value is significantly increased, and the variation range is between -0.001 and 0.0015 . In the central and southern regions, there is a near EW direction average curvature variation zone. The contour lines around them are mostly beaded. Even the maximum and minimum values of the average curvature are 0.00035 and -0.00025 , respectively. The overall mean curvature of the south does not change much, and is mainly concentrated in -0.000025 to 0.000025 . However, there is a significant change in the average curvature of the southeast region. The average curvature range is between -0.0001 and 0.0002 .

The isolines in the figure are mainly distributed between positive and negative phases in the NNW–SSE trend and extend along the NNE direction. The No. 3 coal seam folds in this area are mainly arranged between anticlines and synclines in the NNE direction. The isolines are extremely dense near the axis trace, which indicates that the coal seam elevation changes greatly, which well reflects the fold characteristics in this area. Among them, there are some NNW direction and near EW direction extensions of the contour lines, which indicates that the area on the basis of an NNE direction fold also developed some NNW direction and near EW direction secondary folds.

The structure northwest of the study area is relatively simple and the deformation is weak. The eastern fractures are relatively developed, which have great influence on curvature. They are in the weak fold deformation zone. A large nearly EW direction Taohu syncline is developed in the central and southern regions, which has a certain impact on the surrounding areas. It causes a large change in the average curvature. The southern structure is relatively simple. Some large folds are developed, and the average curvature changes little. However, several large NE direction fractures are developed in the southwest, which have a great influence on the average curvature of the surrounding areas. This is consistent with the construction of the mean curvature diagram reaction.

4.2.3. Gaussian Curvature

The average curvature has a good response to the shape of the study area, but the response to deformation is insufficient. In the Gaussian curvature diagram, the value range of Gaussian curvature is between -1.8×10^{-7} and 4×10^{-8} , and the curvature value is generally small. Most areas of Gaussian curvature are concentrated between -1×10^{-8} and -2.6×10^{-23} , which indicates that the bending degree of the coal seam is relatively small. It is consistent with the actual coal seam inclination. The curvature value of the northwest region is small, and they are concentrated in -2.6×10^{-23} . The change range is small, and the contour only has some changes in the local area. The change range of curvature value in the eastern region is obviously increased. The Gaussian curvature range is between -3×10^{-8} and 2×10^{-8} . There is a Gaussian curvature change zone in the central and southern regions. The maximum value of Gaussian curvature 4×10^{-8} and the minimum value -1.8×10^{-7} appear here, and the contour around them is mostly beaded. There is little change in the overall Gaussian curvature in the south, and the Gaussian curvature is concentrated in -2.6×10^{-23} . However, there is a significant change in the Gaussian curvature in the southeast region. The curvature range is between -3×10^{-8} and 3×10^{-8} .

The isolines in the figure are mainly distributed between positive and negative phases in the NNW–SSE trend, and extend along the NNE direction. The No. 3 coal seam folds in this area are mainly arranged between anticlines and synclines in the NNE direction. Among them, there are some isolines extending in the NNW direction and near EW direction, which indicates that some secondary folds in the NNW direction and near EW direction are developed on the basis of the NNE direction folds in this area. Three kinds of fold superposition interference on each other, constituting the tectonic form of this area.

The northwest structure of the study area is relatively simple and deforms weakly. They develop into some regularly arranged anticlines and synclines. The eastern fracture is relatively developed, which has a great influence on the Gaussian curvature. It is in the weak fold deformation area, and the coal seam deformation is obvious. A large-scale nearly EW direction Taohe syncline is developed in the central and southern regions. It leads to a large change in Gaussian curvature. The surrounding area is also greatly affected, and the coal seam has obvious deformation. The southern structure is relatively simple, and some large folds are developed. The change in Gaussian curvature is small, and the deformation of the coal seam is weak. However, several large NE direction fractures are developed in the southwest, which have great influence on the Gaussian curvature of the surrounding area, and the coal seam also has certain deformation.

4.2.4. Structural Curvature Characteristics

The curvature value of the coal seam in the Yangquan mining area is generally small. It indicates that the overall bending degree of the coal seam in the Yangquan mining area is small. It is consistent with the small overall dip angle of strata in the whole area. The dense contour in the figure indicates that the curvature changes greatly and the bending deformation of the coal seam is relatively high. The dense contour lines in the four maps are also concentrated in the NNW–SSE trend, which shows that the anticline and syncline are distributed in this direction, resulting in a large degree of coal seam bending in this area. The contour line mainly extends along the NNE direction, and the individual contour lines are the NW direction and nearly EW direction. It shows that the main direction of the fold is in the NNE direction, which is superimposed with the NW and nearly EW direction folds developed between them. The dome structure, tectonic basin and saddle structure are distributed in various mines in the study area. They are consistent with the structural characteristics of the Yangquan mining area.

The four curvature maps show that the northwest structure is relatively simple. The deformation is weak, and some regularly arranged anticlines and synclines are developed. The eastern fracture is more developed and has a great influence on the curvature. It is in the weak fold deformation area, and the coal seam deformation is obvious. A large nearly EW direction Taohe syncline is developed in the central and southern parts, resulting in a large change in curvature. The surrounding area is also greatly affected, and the coal seam has obvious deformation. The southern structure is relatively simple, and some large folds are developed. The curvature changes are small, and the deformation of the coal seam is weak. However, several large NE direction fractures are developed in the southwest. They have a great influence on the curvature of the surrounding area, and the coal seam also has a certain deformation.

5. Quantitative Evaluation of Structure Fractal

The phenomenon of self-similarity in geological structures is quite common. The microscopic faults, joints and faults have statistical self-similarity in geometry, kinematics and dynamics, which reflects the application of fractal thought in structural research and becomes an important method for the quantitative evaluation of structural complexity in bore fields.

5.1. Dimension Measurement

There are several practical definitions of dimension in the application of fractal geometry [41]:

1. Similarity Dimension (D_s): For Self-Similar Sets “F”:

$$D_s(F) = \ln m / \ln(1/c) \quad (16)$$

If the research target with self-similarity can be divided into m units, each unit can be similar to the whole according to the specific proportional coefficient “ c ”. “ m ” is the number of similar subsets. “ c ” is the proportional coefficient.

2. Capacity Dimension (D_k): Assuming the Number of Squares in “F” is “ $N(\varepsilon)$ ”, We Define Capacity Dimension “ D_k ”:

$$D_k(F) = \ln N(\varepsilon) / \ln(1/\varepsilon) = -\ln N(\varepsilon) / \ln(1/\varepsilon) \quad (17)$$

For fracture grids, the number of grids called “ $N(\varepsilon)$ ” containing fracture traces is counted by using the grid with edge length called “ ε ”. The corresponding number of grids “ $N(\varepsilon_i)$ ” is obtained by continuously reducing the grid size to “ ε_i ”. In the $\ln \varepsilon - \ln N(\varepsilon)$ double logarithmic coordinate system, a fitting curve can be obtained. The slope of the straight line is the capacity dimension called “ D_k ” of the fracture system.

5.2. Fractal Evaluation of Construction Complexity

According to the fracture data on the coal seam mining engineering drawing (Figure 9), the grid covering method is used to count the fracture structure in the study area and calculate the capacity dimension. On this basis, the fractal dimension contour map is made to evaluate the complexity.

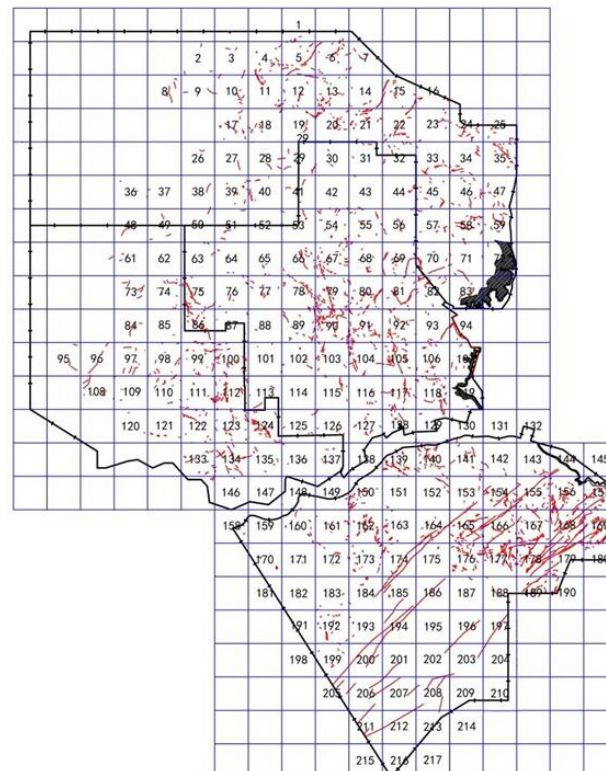


Figure 9. Division map of dstructural fractal evaluation unit in research area.

Calculation and Evaluation of Fracture Capacity Dimension

According to the side length of 1000×1000 m, 500×500 m, 250×250 m and 125×125 m, the well-field tectonic units are divided into several grade grids. The number of grids containing fracture traces in each unit is counted. The analysis of double logarithmic linear regression results is shown in Figure 10. Based on the capacity dimension and coordinate of each unit center point, the data are interpolated and encrypted by the Kriging interpolation method. The plane distribution of fracture capacity in Figure 11 is obtained. It can be seen from the diagram that the fracture capacity dimension value basically reflects the complexity of the fracture structure of No. 3 coal seam in the study area. The capacity dimension of the well-field fracture is mostly between 0.6 and 1.6, which indicates that the complexity of the well-field fracture structure has obvious indigenous heterogeneity. From the analysis of the complexity of the fault structure of the whole mine, it can be seen that the fractures in the dense development area of the fracture structure in the southeast of the study area are the most developed and dense. The fractal dimension contour reaches two. There are also four areas where the fractures are more densely developed. The fracture structure development in other areas is relatively simple.

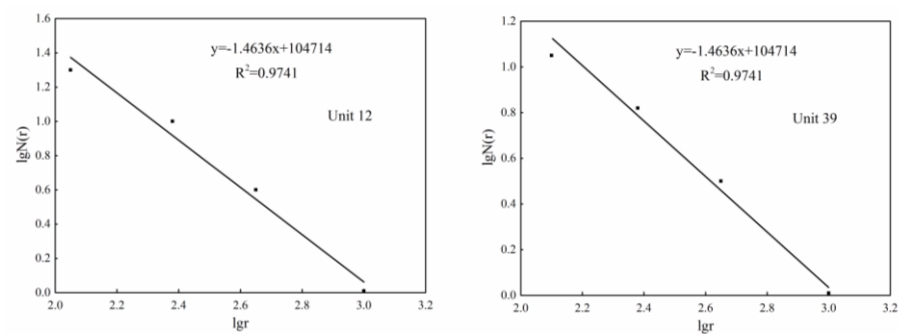


Figure 10. Double logarithmic linear fitting of statistical data of some units.

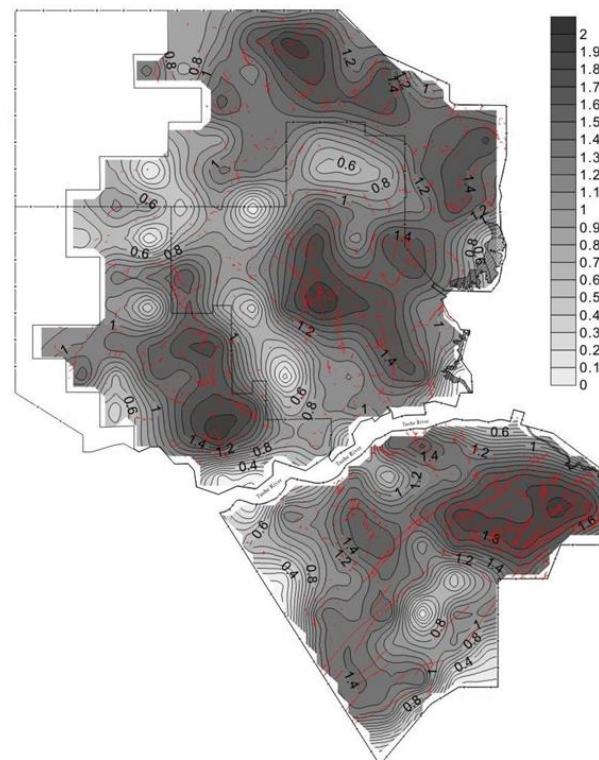


Figure 11. Plane distribution map of regional fracture capacity dimension.

6. Analysis of Fold Neutral Surface

Neutralizing Surface Effect

A single rock layer or a set of rock layers bonded firmly to each other will appear as a neutral surface under the action of longitudinal bending fold. The rock layer has completely different stress states on the neutral surface and below, as shown in Figure 12. The fold strata above the neutral plane of anticline are subjected to tension. The thickness of ductile strata becomes thinner, while the brittle strata generate tensile fracture surfaces. The fold strata below the neutral surface of the anticline are squeezed. The ductile strata move and thicken to the core of the anticline. The brittle strata produce compressive fractures. The stress condition of syncline is opposite to anticline. In addition, the stress effect on the anticline and syncline increases with the increase in the distance from the rock stratum to the neutral plane [42–44].

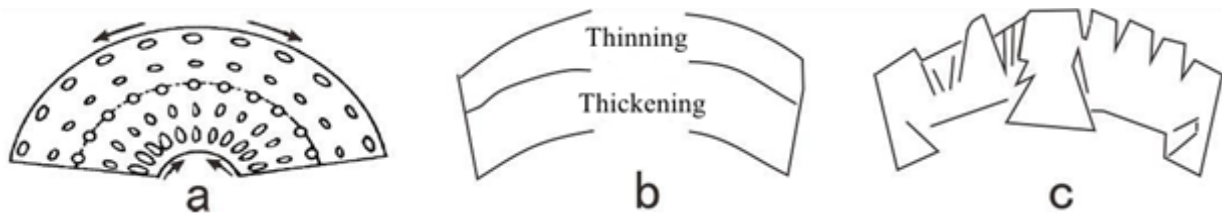


Figure 12. Deformation characteristics under longitudinal-bending fold. (a) Strain state of longitudinal bending. (b) Deformation of ductile layer. (c) Fracture deformation of brittle layer.

Predecessors have carried on the theoretical derivation to determine the simplified cylindrical fold neutral plane position. Formula (18), derived by Gu et al. [45], is widely used.

$$a = \frac{\sum_{i=1}^n \frac{E_i}{1-\mu_i^2} h_i |2h - h_i - 2 \sum_{j=0}^{i-1} h_j|}{2 \sum_{i=1}^n \frac{E_i}{1-\mu_i^2} h_i} \quad (18)$$

In the formula: “a” is the distance from the neutral surface to the lower surface of the independent deformation layer. “ h_i ” is the thickness of each single layer. “ E_i ” is Young’s modulus of each single layer. “h” is total thickness of the independent deformation layer.

Due to the different mineral compositions, porosities, textures, structures, temperatures, water contents, humidity fields and other factors, the elastic modulus and Poisson’s ratio of the same rock layer in different locations in the same area are also different, but the change range is not large. The mechanical properties of the coal (rock) layer are as follows: Table 1.

Table 1. Table of mechanical properties of coal (rock) layer in Yangquan Xinjing Mine.

Lithology	Young’s Modulus ($\times 100$ Mpa)	Poisson Ratio
Mudstone	38	0.3
Limestone	398	0.18
Kern stone	193	0.1
Medium grained sandstone	257	0.12
Post office box stone	288	0.12
Siltstone	101	0.15
Coal	29	0.79

The coal measures and the upper–lower deformed strata in the mine are divided into three sections. The first section is dominated by sandstone. The second section is mudstone, sandy mudstone and sandstone with coal seam. The third section is sandstone and limestone. The mechanical properties of the strata between the first and second sections are quite different from the mechanical properties of the strata between the second and third sections. They all have bending and sliding effects, and they can be divided into

three independent deformed strata. The second section is the main research target. The characteristics of its comprehensive stratigraphic parameters are shown in Table 2.

Table 2. Comprehensive stratigraphic parameters characteristics.

Group	Serial Number	Lithology	Thickness	Young's Modulus ($\times 100$ Mpa)	Poisson Ratio	
Lower stone box group	1	Mudstone, fine sandstone	44	38	0.3	
	2	Grit stone	6	193	0.1	
Shanxi formation	3	Sandy mudstone, mudstone	9.5	38	0.3	
	4	1# coal	0.36	29	0.79	
	5	Fine sandstone and silty mudstone	3.67	163	0.21	
	6	2# coal	0.46	29	0.79	
	7	Sandy mudstone	5.1	38	0.3	
	8	Medium sandstone	5.95	257	0.12	
	9	Silty mudstone	3.42	38	0.3	
	10	3# coal	2.33	29	0.79	
	11	Fine sandstone and silty mudstone	4.59	163	0.21	
	12	4# coal	0.33	29	0.79	
	13	Silty mudstone	4.85	38	0.3	
	14	5# coal	0.25	29	0.79	
	15	Silty mudstone	3.15	38	0.3	
	16	Fine sandstone, medium sandstone	4.96	272.5	0.12	
	17	Silty mudstone	1.13	38	0.3	
	18	6# coal	1.38	29	0.79	
	19	Siltstone	3.65	101	0.15	
	20	Coarse sandstone, fine sandstone	7.71	240.5	0.11	
	Taiyuan Group III	21	Black mudstone	6.33	38	0.3
		22	8# coal	1.73	29	0.79
23		Silty mudstone	5	38	0.3	
24		Medium sandstone	8.15	257	0.12	
25		Silty mudstone	2.5	38	0.3	
26		9# coal	1.46	29	0.79	
27		Silty mudstone, mudstone	4.7	38	0.3	
28		Fine sandstone	5.8	288	0.12	
29		Black mudstone	4.1	38	0.3	
Taiyuan Group II	30	Limestone	2.5	398	0.18	
	31	Black mudstone	1.23	38	0.3	
	32	11# coal	0.3	29	0.79	
	33	Black mudstone	1.5	38	0.3	
	34	Fine sandstone	4.87	288	0.12	
	35	Mudstone	4.4	38	0.3	
	36	12# coal	1.13	29	0.79	
	37	Silty mudstone	1.12	38	0.3	
	38	Fine sandstone	2.9	288	0.12	
	39	Mudstone	1.86	38	0.3	
	40	Limestone	4.69	398	0.18	
	41	Mudstone	0.58	38	0.3	
	42	13# coal	0.74	29	0.79	
	43	Silty mudstone	2.76	38	0.3	
	44	Fine sandstone	7.25	288	0.12	
	45	Silty mudstone	4.6	38	0.3	
	46	Limestone, mudstone	9.16	218	0.24	
Taiyuan Group I	47	14# coal	0.1	29	0.79	
	48	Mudstone	2.05	38	0.3	
	49	15# coal	6.14	29	0.79	
	50	Sandy mudstone	2.05	38	0.3	
	51	Coal below 15#	2	29	0.79	
	52	Sandy mudstone	3.11	38	0.3	

The comprehensive strata of the mine reflect the overall situation of the strata. Taking $n = 52$ into Equation (18), $a = 91.07$ m is calculated by computer. It indicates that the neutral surface of the mine is in the third section of the Taiyuan formation as a whole. The No. 3 coal seam is above the neutral surface, and the distance from the neutral surface is 47.74 m.

7. Conclusions

In this paper, we choose the No. 3 coal seam of the main coal seam in the Yangquan mining area for the research object. According to the structural characteristics of the mine, the fractal dimension, structural curvature, trend surface and fold neutralization surface analysis methods are used to quantitatively evaluate the structural development characteristics of the mine. The main conclusions are as follows:

- (1) Trend surface reflects that the monoclinic structure is high in the NE direction and low in the SW direction, and the dip angle is small. The residual map reflects the morphology of fold development. The zero line in the three residual maps better shows the structural morphology of the mine with an NNE–NE trend distribution as the main feature.
- (2) The high-value area of maximum curvature and the low-value area of minimum curvature of the coal seam-banded and -beaded distribution in the Yangquan mining area have a good indication for the development of syncline and anticline, respectively. The average curvature has a good response to the morphology of fold structure, and the Gaussian curvature also has a good response to the morphology of fold structure.
- (3) From the analysis of the complexity of the fracture structure in the mining area, it can be seen that the fractures in the dense development area of the fracture structure in the southeast of the study area are the most developed and dense. The fractal dimension contour reaches two. There are also four areas where the fractures are more densely developed. The fracture structure development in other areas is relatively simple.
- (4) In terms of the position of the neutral surface of the mine, it is located in the third section of the Taiyuan formation as a whole. The No. 3 coal seam is above the neutral surface, and the distance from the neutral surface is 47.74 m.

Author Contributions: Conceptualization, Z.Y.; Data curation, Y.P. All authors have read and agreed to the published version of the manuscript.

Funding: This research received no external funding.

Informed Consent Statement: Informed consent was obtained from all subjects involved in the study.

Data Availability Statement: The data used to support the findings of this study are available from the corresponding author upon request.

Conflicts of Interest: The authors declare no conflict of interest.

References

1. Wang, E.Y.; Yi, W.X.; Li, Y.B. *The distribution and Genetic Mechanism of Tectonic Coal in North China Plate*; Science Press: Beijing, China, 2015.
2. Wang, K.; Du, F. Coal-gas compound dynamic disasters in China: A review. *Process Saf. Environ. Prot.* **2020**, *133*, 1–17. [[CrossRef](#)]
3. Wang, L.; Zheng, S.; Zhao, W.; Chen, D.P.; Zhu, Z.B. Study on difference and control factors of coal and gas outburst disasters in Huaibei Coalfield. *Coal Sci. Technol.* **2020**, *48*, 75–83.
4. Wang, T.X.; Yu, C.; Wei, B.; Li, R.M.; Wang, Q.W.; Yang, S.G.; Jaing, T.; Wang, C.T. Structural styles and their control effect on Jurassic coalfield in Xinjiang. *J. China Coal Soc.* **2017**, *42*, 436–443.
5. Wang, K.; Guo, Y.; Wang, G.; Du, F. Seepage and Mechanical Failure Characteristics of Gas-bearing Composite Coal-Rock Under True Triaxial Path. *J. China Coal Soc.* **2022**, 1–12. [[CrossRef](#)]
6. Wang, S.M. Ordos Basin tectonic evolution and structural control of coal. *Geol. Bull. China* **2011**, *30*, 544–552.
7. Lin, D. *Research on the Geological Structure Characteristics and Complexity Evaluation of Sunan Mining Area*; Anhui University of Science and Technology: Huainan, China, 2015.
8. Zhao, M.P. Application of structural analysis method in mine geological structure prediction. *J. Fuxin Min. Inst.* **1991**, 68–71.
9. Xu, F.Y.; Long, S.R.; Xia, Y.C.; Xie, D.K. Quantitative evaluation and prediction of mine geological structure. *J. China Coal Soc.* **1991**, *16*, 93–101.

10. Xu, F.Y.; Zhu, X.S.; Wang, G.L.; Ma, X.H. The quantitative research on the paleotectonic stress field and its control to coal and gas outburst. *Sci. Geol. Sin.* **1995**, *30*, 71–84.
11. Xia, Y.C.; Xu, F.Y. Application of grey Correlation Analysis in fuzzy comprehensive evaluation. *J. Xian Min. Inst.* **1991**, *11*, 44–50.
12. Xia, Y.C.; Hu, M.X.; Chen, L.W. Gmdh-bp evaluation and prediction method of mine structure and its application. *J. China Coal Soc.* **1997**, *22*, 466–470.
13. Xia, W.C. Research progress on quantitative prediction technology of mine structure. *Geol. Prospect.* **2001**, *27*, 61–63.
14. Zhu, X.S.; Xu, F.Y. The controlling effect of tectonic stress field and its evolution on coal and gas outburst. *J. China Coal Soc.* **1994**, *19*, 303–314.
15. Zhu, X.S.; Xu, F.Y.; Li, Q.Y. Development characteristics and influencing factors of damaged coal in Nantong mining area. *Coal Geol. Explor.* **1996**, *24*, 28–32.
16. Zhang, Z.M.; Zhang, Y.G. Investigation into coal-gas outburst occurred in Daping Coalmine, by using theories of gas-geology. *J. China Coal Soc.* **2005**, *30*, 137–140.
17. Zhang, Z.M.; Zhang, Y.G. *Gas Geological Law and Gas Prediction*; China Coal Industry Publishing House: Beijing, China, 2005.
18. Zhang, Z.M.; Zhang, Y.G.; Wei, X.J. *Compilation of Three-Level Gas Geological Map of Coal Mine*; China Coal Industry Publishing House: Beijing, China, 2007.
19. Song, Y.; Zhao, M.J.; Liu, S.B.; Wang, H.Y.; Chen, Z.H. The influence of structural evolution on the enrichment degree of coalbed methane. *Chin. Sci. Bull.* **2005**, *50*, 1–5. [[CrossRef](#)]
20. Han, J.; Zhang, H.W.; Song, W.H.; Li, S.; Lan, T.-W. Coal and gas outburst mechanism and risk analysis of tectonic concave. *J. China Coal Soc.* **2011**, *36*, 108–113.
21. Zhang, Z.M.; Wu, Y. *Chinese Coalmine Gas Geological Law and Mapping*; China University of Mining and Technology Press: Xuzhou, China, 2014.
22. Zhang, Z.M.; Wu, Y. Tectonic-level-control rule and area-dividing of coalmine gas occurrence in China. *Earth Sci. Front.* **2013**, *20*, 237–245.
23. Han, J.; Zhang, H.W.; Zhang, P.T. Nappe structure's kinetic features and mechanisms of action to coal and gas outburst. *J. China Coal Soc.* **2012**, *37*, 247–252.
24. Du, F.; Wang, K.; Zhang, X.; Xin, C.; Shu, L.; Wang, G. Experimental study of coal-gas outburst: Insights from coal-rock structure, gas pressure and adsorptivity. *Nat. Resour. Res.* **2020**, *29*, 2481–2493. [[CrossRef](#)]
25. Gao, K.; Liu, Z.G.; Liu, J.; Deng, D.S.; Kang, Y.; Haung, K.F. Physical and mechanical characteristics of tectonic soft coal and their effects on coal and gas outburst. *China Saf. Sci. J.* **2013**, *23*, 129–133.
26. Zhang, C.H.; Liu, Z.G.; Liu, J.; Cai, F.; Zhang, S.C. Physical scale modeling of mechanical characteristics of outburst induced by closed geological structure. *J. China Univ. Min. Technol.* **2013**, *42*, 554–559.
27. Jia, T.R.; Feng, Z.D.; Wei, G.Y.; Ju, Y.W. Shear deformation of fold structures in coal measure strata and coal-gas outbursts: Constraint and mechanism. *Energy Explor. Exploit.* **2018**, *36*, 185–203. [[CrossRef](#)]
28. Cao, D.Y.; Ning, S.Z.; Guo, A.J. *Tectonic Framework of Coalfields and Tectonic Control of Coalseams in China*; Science Press: Beijing, China, 2018.
29. Ju, Y.W.; Wei, M.M.; Xue, C.D. Control of basin-mountain evolution on the occurrence of deep coal and coalbed methane in North China. *J. China Univ. Min. Technol.* **2011**, *40*, 390–398.
30. General Administration of Coal Geology of China. *Sedimentary Environment and Coal Accumulation Law of Late Permian Coal-Bearing Strata in Western Guizhou, Southern Sichuan and Eastern Yunnan*; Chongqing University Press: Chongqing, China, 1996.
31. Gao, R. Coal seam thickness variation law and its controlling factors in Xin'an coalfield, western Henan. *Coal Geol. Explor.* **2011**, *39*, 102–110.
32. Wang, Z. Analysis of coal accumulation sedimentary environment and coal thickness change in Guozhuang mine field. *Coal Sci. Technol.* **2010**, *38*, 90–98.
33. Deng, G. Discussion on coal forming environment and coal accumulation law of late Permian coalfield in eastern Sichuan. *Sichuan J. Geol.* **1994**, *14*, 35–40.
34. Feng, Z. Stratigraphic sequence and coal accumulation characteristics of Longtan formation in Guxu mining area, southern sichuan. *Sichuan J. Geol.* **2010**, *30*, 46–52.
35. Liu, F. Analysis of sedimentary environment and coal forming conditions of Longtan Formation in Baibu Prospecting Area. *Coal Geol. China* **2008**, *20*, 39–46.
36. Zhong, M. Sedimentary environment and coal accumulation of Longtan formation in Moxinpo, Chongqing. *J. Henan Polytech. Univ.* **2011**, *30*, 202–210.
37. Deng, G. Sedimentary characteristics and coal accumulation law of Longtan formation in Yanjing mining area, Libixia back slope, Chongqing. *Coal Geol. China* **2007**, *19*, 198–206.
38. Wei, Y. *Sedimentary Characteristics and Coal Forming Environment of Songshutou Coal-Bearing Strata in Urumqi*; Coal Geology of China: Xinjiang, China, 2011; Volume 23, pp. 124–130.
39. Chen, M. Sedimentary environment and coal accumulation law of Guanzhai well field. *Coal Geol. China* **2008**, *20*, 301–309.
40. Cui, J. Coal seam characteristics and coal accumulation environment analysis of Shanxi formation in Zhaigou field, Xinmi coalfield. *Coal Geol. China* **2012**, *24*, 58–66.

41. Du, F.; Wang, K. Unstable failure of gas-bearing coal-rock combination bodies: Insights from physical experiments and numerical simulations. *Process Saf. Environ. Prot.* **2019**, *129*, 264–279. [[CrossRef](#)]
42. Shen, J.; Fu, X.H.; Qin, Y.; Liu, Z. Control action of structural curvature of coal seam floor on coalbed gas in the No.8 Coal Mine of Pingxiangshan. *J. China Coal Soc.* **2010**, *35*, 586–589.
43. Zhang, W.Q.; Sun, M.; An, W.; Ma, Y.F. Study on the Discrimination of Water Inrush from Deep-well Floor Based on Fuzzy Neural Network. *China Saf. Sci. J.* **2009**, *19*, 61–65.
44. Rao, J.J.; Zhang, W.T.; Liu, Q.M. Study on the Control of Stress on Geothermal in Anticlinal Strata. *J. Anhui Univ. Sci. Technol.* **2021**, *40*, 46–52.
45. Gu, H.X.; Fu, X.H.; Ji, M.; Chen, L. Locating neutral surface of fold and its application in Laohe syncline in Liupanshui area. *Coal Geol. Explor.* **2011**, *39*, 11–14.